Effect of yttrium on dynamic strain aging of vanadium alloys

ID: 15-260

EFFECT OF YTTRIUM ON DYNAMIC STRAIN AGING OF VANADIUM ALLOYS

Takeshi Miyazawa[a]*, Takuya Nagasaka[a,b], Yoshimitsu Hishinuma[a,b], Takeo Muroga[a,b], Yanfen Li[b], Yuhki Satoh[c], Sawoong Kim[c] and Hiroaki Abe[c]

[a]The Graduate University for Advanced Studies: Toki, Gifu 509-5292, Japan

[b]National Institute for Fusion Science: Toki, Gifu 509-5292, Japan

[c]Institute for Materials Research, Tohoku University: Sendai 980-8577, Japan

* Corresponding author, Tel. +81-572-58-2332, Fax. +81-572-58-2676, email: miyazawa.takeshi@LHD.nifs.ac.jp

Abstract:

In order to improve the performance of vanadium alloys for fusion reactors, yttrium (Y) was added to reduce the interstitial O in the matrix by enhanced precipitation with Y. Effect of Y on interstitial C, N and O, however, remains to be investigated since they affect mechanical and fracture properties for vanadium alloys by pinning dislocations, such as dynamic strain aging (DSA). In this study, tensile tests were carried out on annealed V-4Cr-4Ti and V-4Cr-4Ti-Y alloys from 473 to 1073 K at strain rates ranging from 6.67×10^{-5} to 6.67×10^{-1} s^{-1} to investigate the performance of DSA. In the case of high-purity alloys, DSA regime was narrowed due to Y addition and the reduction in O content. In the case of O doped V-4Cr-4Ti alloys, DSA regime was also narrowed. This may be because the enhanced Ti-O precipitation reduced the O level in the matrix. Also, coarse precipitates (< 500 nm) were observed in O doped V-4Cr-4Ti-Y alloy. Y might enhance the coarsening of Ti-precipitates. From activation energies for DSA, the diffusion of C and O is considered to induce the observed DSA. Y does not influence the diffusion of C and O, and might enhance the nucleation to form coarse precipitates.

Main text:

EFFECT OF YTTRIUM ON DYNAMIC STRAIN AGING OF VANADIUM ALLOYS

Takeshi Miyazawa, Takuya Nagasaka, Yoshimitsu Hishinuma, Takeo Muroga, Yanfen Li, Yuhki Satoh, Sawoong Kim and Hiroaki Abe

1. Introduction

V-4Cr-4Ti alloys are recognized as attractive blanket structural materials for fusion reactor systems because they exhibit low neutron-induced activation, high-temperature strength and high-thermal stress factor required for high-temperature systems [1]. The mechanical behavior of V-4Cr-4Ti and of body-centered cubic (BCC) alloys in general is strongly influenced by interstitial carbon (C), nitrogen (N) and oxygen (O) [2]. It is widely recognized that the reduction of these impurities is essential for maintaining workability [3] and weldability [4]. It has been reported that a small addition of yttrium (Y) was effective to reduce interstitial O and improve ductility after neutron irradiation without degradation of low-temperature impact properties [5-7]. While Y addition moderates the hardening induced by O, it can also degrade high-temperature strengths [8]. The deformation behavior of V-4Cr-4Ti alloys during tensile tests typically at temperatures ranging from 573 to 1023 K was shown to exhibit dynamic strain aging (DSA), which is manifested by oscillations in the flow stress as serrations on the stress-strain curves. The formation of Cottrell atmospheres composed of interstitial C, N and O at locked dislocations results in DSA. DSA is

considered an undesired phenomenon because it results in a loss of ductility and negative strain rate sensitivity, thus adversely affecting mechanical and fracture properties [9]. A previous study [8] reported that total elongation (TE) for V-4Cr-4Ti alloys decreased in DSA regime. At high-temperature region above 973 K, Y addition suppressed DSA and improved TE. It, however, induced the reduction in ultimate tensile strengths (UTS). Y could form coarse inclusions and then these inclusions could induce the nucleation and growth of microcracks leading to fracture. The purpose of this study is to deduce the mechanism of Y influence on DSA by systematic characterization of the tensile properties and microstructures, and by kinetic analyses.

2. Experiment

Results of chemical analysis for V alloys used in this study are shown in Table I. V-4Cr-4Ti-0.019O is the reference V-4Cr-4Ti alloy, NIFS-HEAT-2, which was fabricated by electron beam melting and vacuum arc re-melting in 166 kg-scale [10]. V-4Cr-4Ti-0.18O was 30 g-scale button and fabricated by arc-melting. V-4Cr-4Ti-Y alloys were fabricated by a levitation melting process in 15 kg-scale [5]. Two types V-4Cr-4Ti-Y alloys were prepared; one was a high-purity alloy (V-4Cr-4Ti-0.11Y-0.009O), and the other was an alloy doped with oxygen (V-4Cr-4Ti-0.06Y-0.27O). Miniature tensile specimens with a gauge size of 5 x 1.2 x 0.25 mm^3, called SSJ type, were used for tensile tests. The tensile specimens were annealed at 1273 K for 7.2 ks for V-4Cr-4Ti alloys, and at 1223 K for 3.6 ks for the V-4Cr-4Ti-Y alloys in a vacuum better than

1×10^{-4} Pa. Tensile tests were carried out from 473 to 1073 K in a vacuum better than 1×10^{-4} Pa. Specimens were held at the test temperature for 15 min before starting the test. The initial strain rate ranged from 6.67×10^{-5} to 6.67×10^{-1} s^{-1}. Data on engineering stress and strain were acquired digitally at rates from 100,000 points per second (pps) for tests conducted at 6.67×10^{-1} s^{-1} strain rate to 10 pps at 6.67×10^{-5} s^{-1} strain rate. Microstructural observations were carried out using a transmission electron microscope (TEM).

3. Results

3.1. Tensile tests

Figure 1 shows diagrams for the DSA regime for V-4Cr-4Ti and V-4Cr-4Ti-Y alloys as a function of strain rate and temperature. Serrations were observed at a moderate temperature and a certain strain rate region, where temperature and strain rate correspond to the diffusion of solute atoms, v_i, and dislocation velocity, v_d, respectively. When $v_i > v_d$, solute atoms can interact with dislocations and then serrations appear in the work-hardening regimes of the stress-strain curves, which is indicated as DSA regime in the figure1. For low-temperatures and high-strain-rates, serrations did not appear because of $v_i < v_d$. Serrations disappeared at high-temperatures because solute atoms undergo rapid thermal detrapping at the dislocations.

It must be noted that there was a difference in the observed DSA regimes between

V-4Cr-4Ti-0.019O and V-4Cr-4Ti-0.11Y-0.009O for high-temperatures where serrations disappear. Serrations for V-4Cr-4Ti-0.019O appeared at higher temperature than those for V-4Cr-4Ti-0.11Y-0.009O. The DSA regime was narrowed due to Y addition and the reduction in O content. Although V-4Cr-4Ti-0.18O was an alloy doped with high O content, the DSA regime for V-4Cr-4Ti-0.18O was narrower than that for V-4Cr-4Ti-0.019O. The DSA regime for V-4Cr-4Ti-0.18O is thought to be almost identical to that for V-4Cr-4Ti-0.06Y-0.27O.

3.2. TEM observation

Figure 2 shows the TEM microstructures of the alloys. Coarse precipitates were barely observed in V-4Cr-4Ti-0.11Y-0.009O because of extremely small numbers of these precipitates. Small precipitates with 200 nm or less in diameter were observed in V-4Cr-4Ti-0.019O, V-4Cr-4Ti-0.18O and V-4Cr-4Ti-0.06Y-0.27O. From a comparison between V-4Cr-4Ti-0.019O and V-4Cr-4Ti-0.18O, the number of small precipitates increased with increasing O content. Various precipitates were also observed in V-4Cr-4Ti-0.06Y-0.27O. These precipitates are classified into small precipitates and large precipitates with 500 nm or more in diameter. Small and large precipitates were identified as Ti-rich and V-rich precipitates, respectively, as shown in Fig. 3. While Y was not identified in small and large precipitates in V-4Cr-4Ti-0.06Y-0.27O based on the TEM energy dispersive X-ray (EDX) results, Y was only identified in coarse precipitates in V-4Cr-4Ti-0.11Y-0.009O. Coarse precipitates are considered to be Y_2O_3 type inclusions.

4. Discussion

4.1. Effect of Y addition on DSA regime

Dynamic strain aging is induced by the diffusion of solute atoms, especially interstitial O in vanadium [11], to dislocations to form Cottrell atmospheres that become barriers to dislocation movement during plastic deformation. The reduction of interstitial O reduces the DSA effect and so narrows the observed DSA regime. Fig. 1 showed the DSA regime was narrowed due to Y addition and the reduction in O content in the case of high-purity alloys, V-4Cr-4Ti-0.019O and V-4Cr-4Ti-0.11Y-0.009O. It is, therefore, thought that interstitial O content for V-4Cr-4Ti-0.11Y-0.009O is lower that for V-4Cr-4Ti-0.019O. Y is suggested to trap O in the matrix more strongly than Ti, reducing O level in the matrix. However the present TEM observation showed only very low density of Y_2O_3 particles. It may be possible that Y_2O_3 particles were distributed heterogeneously. In the case of O doped alloys (V-4Cr-4Ti-0.18O and V-4Cr-4Ti-0.06Y-0.27O), Ti might enhance the formation of fine precipitates, which can absorb interstitial O. Y might enhance the coarsening of Ti-precipitates. Ultrafine Y_2O_3 forms in high density and then Y might enhance nucleation for precipitation because Y_2O_3 becomes a nucleus of precipitates, or enhance growth for precipitation due to the reduction in interfacial surface energy of precipitates by segregation of Y_2O_3 [12,13]. A further study of microstructural observation and distribution of Y in V-4Cr-4Ti-Y alloys will be carried out.

4.2. Activation energy for the diffusion of solute atoms

Solute atoms movement occurs by diffusion and the solute diffusion rate v_i is given by

$$v_i = \left(FD_o / kT \right) \exp\left(-E / kT \right) \qquad (1)$$

where F = -grad V. V, D_0, k, T and E are the energy of interaction between dislocation and solute atoms, the diffusion coefficient, Boltzmann constant, the absolute temperature and the activation energy for the diffusion of solute atoms, respectively. Assuming the density of mobile dislocations N is constant, the relationship between strain rate dε/dt and dislocation velocity v_d is given as

$$d\varepsilon / dt = Nbv_d \qquad (2)$$

where b is Burgers vector. The condition where the diffusion rate of solute atoms is equal to the dislocation velocity, equation (3) $v_i = v_d$, is considered to be the bounding condition of DSA. Substituting equations (1) and (2) into equation (3) gives

$$\ln\left(T \times d\varepsilon / dt \right) = -\left(E / k \right)\left(1/T \right) + const. \qquad (4)$$

Figure 4 plots data for V-4Cr-4Ti-0.11Y-0.009O in Fig. 1 (b) as the critical condition parameter,

ln(T x dε/dt), on the y-axis and inverse absolute temperature 1/T on the x-axis. According to equation (4), the activation energy for the diffusion of solutes can be estimated from the slope of the bounding line for the DSA regime. It was difficult to obtain activation energy precisely from the bounding line on the high-temperature side, because serrations were observed after necking, where N was no longer constant because of the local generation of dislocations by necking deformation. Table II summarizes the activation energy estimated by the bounding line on the lower-temperature side. Table III shows the data in the literature for the activation energy for diffusion in pure vanadium and V-4Cr-4Ti alloys. The experimental data except for V-4Cr-4Ti-0.18O are close to the data in the literature for C in pure vanadium and O in pure vanadium and V-4Cr-4Ti. The diffusion of C and O is suggested to be the cause of the observed DSA at lower-temperatures. Activation energies were not significantly changed by Y addition. Thus, Y does not influence the diffusion of C and O but reduces DSA regime at higher-temperatures. Hoelzer and Rowcliffe reported that an interaction between interstitial impurities and substitutional Ti (I-S effect) is the primary reason for widening DSA at higher-temperatures [18]. In addition to substitutional Ti, interstitial O strongly interacts with substitutional Y due to a stronger chemical affinity between Y and O than that between Ti and O [19]. Y, therefore, influences DSA at higher-temperatures.

5. Conclusions

The effect of yttrium (Y) on dynamic strain aging (DSA) has been clarified from tensile tests conducted at temperatures ranging from 473 to 1073 K and strain rates ranging from 6.67×10^{-5} to 6.67×10^{-1} s^{-1}.

The temperature range over which DSA was observed was narrowed by Y addition to V-4Cr-4Ti alloys and the reduction in O content. Also, serrations were suppressed due to the reduction in interstitial O content in the matrix caused by the enhanced precipitation. From measured activation energies, the diffusion of C and O induce DSA at lower-temperatures for these alloys. However, Y addition to V-4Cr-4Ti alloys was not observed to have any effect on the diffusion of C and O.

Acknowledgements

The author is grateful to Mr. T. Onda of Onda Kougyo Co., Ltd. for supports in the fabrication of vanadium alloy and to a financial support from Course-by-Course Education Program to Develop Student Research for the Graduate University for Advanced Studies.

References

1. T. Muroga, T. Nagasaka, K. Abe, V.M. Chernov, H. Matsui, D.L. Smith, Z.-Y. Xu and S.J. Zinkle, J. Nucl. Mater., 307-311 (2002) 547-554.
2. T. Nagasaka, H. Takahashi, T. Muroga, T. Tanabe and H. Matsui, J. Nucl. Mater., 283-287 (2000) 816-821.
3. D.R. Diercks and B.A. Loomis, J. Nucl. Mater., 141-143 (1986) 1117.
4. M.L. Grossbeck, J.F. King, D.J. Alexander, P.M. Rice and B.A. Loomis, J. Nucl. Mater., 258-263 (1998) 1369.
5. T. Nagasaka, T. Muroga, T. Hino, M. Satou, K. Abe, T. Chuto and T. Iikubo, J. Nucl. Mater., 367-370 (2007) 823-828.
6. M. Satou, T. Chuto and K. Abe, J. Nucl. Mater., 283-287 (2000) 367-371.
7. T. Chuto, M. Satou, A. Hasegawa, K. Abe, T. Muroga and N. Yamamoto, J. Nucl. Mater., 326 (2004) 1-8.
8. T. Miyazawa, T. Nagasaka, Y. Hishinuma, T Muroga and Y. Li, Fusion Sci. Technol., 60 (2011) 407.
9. I. Charit, C.S. Seok and K.L. Murty, J. Nucl. Mater., 361 (2007) 262-273.
10. T. Nagasaka, T. Muroga, M. Imamura, S. Tomiyama and M. Sakata, Fusion Technology, 39, (2001) 659-663.
11. M. Koyama, K. Fukumoto and H. Matsui, J. Nucl. Mater., 329-333 (2004) 442-446.
12. B. Forbord, W. Lefebvre, F. Danoix, H. Hallem and K. Marthinsen, Scr. Mater., 51 (2004) 333-337.
13. M. Hatakeyama, T. Toyama, Y. Nagai, M. Hasegawa, M. Eldrup and B.N. Singh, Mater. Trans., 49 (2008) 518-521.
14. Metal data book, the Japan Institute of Metals (1993).
15. F.A. Schmidt and J.C. Warner, J. Less-Common Metals., 26 (1972) 325-326.
16. M. Uz, K. Natesan and V.B. Hang, J. Nucl. Mater., 245 (1997) 191-200.
17. Diffusion data base, National Institute for Materials Science.
18. D.T. Hoelzer and A.F. Rowcliffe, J. Nucl. Mater., 307-311 (2002) 596-600.
19. T.H. Okabe, T.N. Deura, T. Oishi, K. Ono and D.R. Sadoway, J. Alloys. Comp., 237 (1996) 150-154.

Table:

Table 1. Chemical composition of the alloys (wt%).

Code	Cr	Ti	Y	C	N	O
V-4Cr-4Ti-0.019O	4.11	4.15	<0.02	0.025	0.009	0.019
V-4Cr-4Ti-0.18O	4.24	4.42	<0.02	0.009	0.018	0.18
V-4Cr-4Ti-0.11Y-0.009O	4.23	4.17	0.11	0.011	0.009	0.009
V-4Cr-4Ti-0.06Y-0.27O	3.87	3.99	0.06	0.010	0.018	0.27

Table 2. Activation energies estimated using the low-temperature DSA bounding line.

Code	Activation energy (kJ/mol)		
	Minimum	Center	Maximum
V-4Cr-4Ti-0.019O	108	114	131
V-4Cr-4Ti-0.18O	137	158	180
V-4Cr-4Ti-0.11Y-0.009O	117	125	134
V-4Cr-4Ti-0.06Y-0.27O	108	114	131

Table 3. Activation energy for diffusion in pure V and V-4Cr-4Ti.

Element	Activation energy (kJ/mol)	Matrix
C	114 (1118-1403 K) [14]	V
N	148 (1923-2098 K) [15]	V
O	123 (1923-2098 K) [15] 130 (623 - 893 K) [16]	V V-4Cr-4Ti
V	308 (1153-1629 K) [14]	V
Cr	270 (1233-1473 K) [14]	V
Ti	285 (1373-1623 K) [17]	V
Y	No data	V

Figure captions:

Fig. 1. DSA regimes for (a) V-4Cr-4Ti-0.019O, (b) V-4Cr-4Ti-0.18O, (c) V-4Cr-4Ti-0.11Y-0.009O and (d) V-4Cr-4Ti-0.06Y-0.27O. Crosses show data for smooth stress-strain curves with no serrations. Closed circles show data for stress-strain curves with serrations. Open circles show data for stress-strain curves with serrations only after necking.

Fig. 2. TEM microstructures of the various V-4Cr-4Ti alloys examined in this study.

Fig. 3. TEM-EDX spectrum for (a) Y-oxide inclusion in V-4Cr-4Ti-0.11Y-0.009O, and (b) small and (c) large precipitates in V-4Cr-4Ti-0.06Y-0.27O.

Fig. 4. Arrhenius plot of critical condition parameter ln (T x dε/dt) versus inverse absolute temperature (1000/T) for V-4Cr-4Ti-0.11Y-0.009O.

Figures:

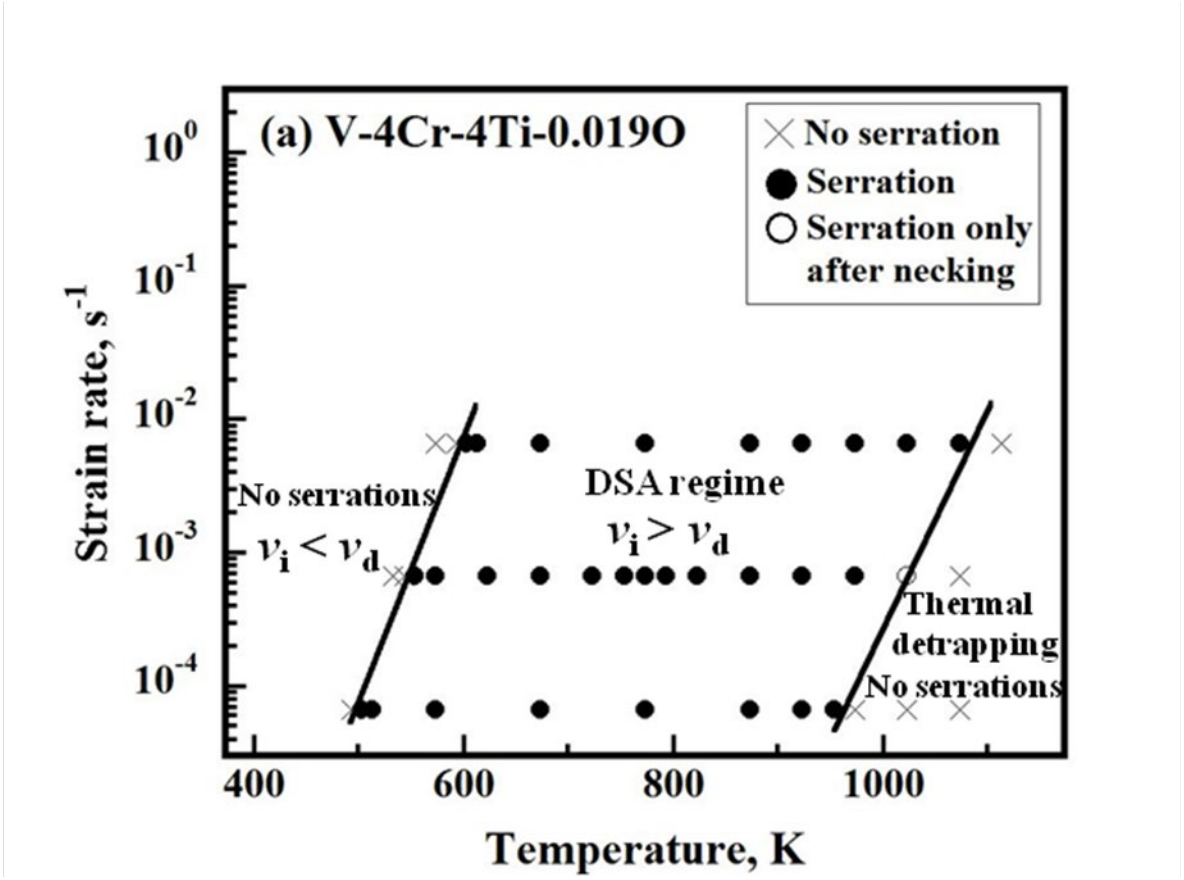
(a) V-4Cr-4Ti-0.019O
No serration
Serration
Serration only after necking
No serrations
$v_i < v_d$
DSA regime
$v_i > v_d$
Thermal detrapping
No serrations
Strain rate, s^{-1}
Temperature, K

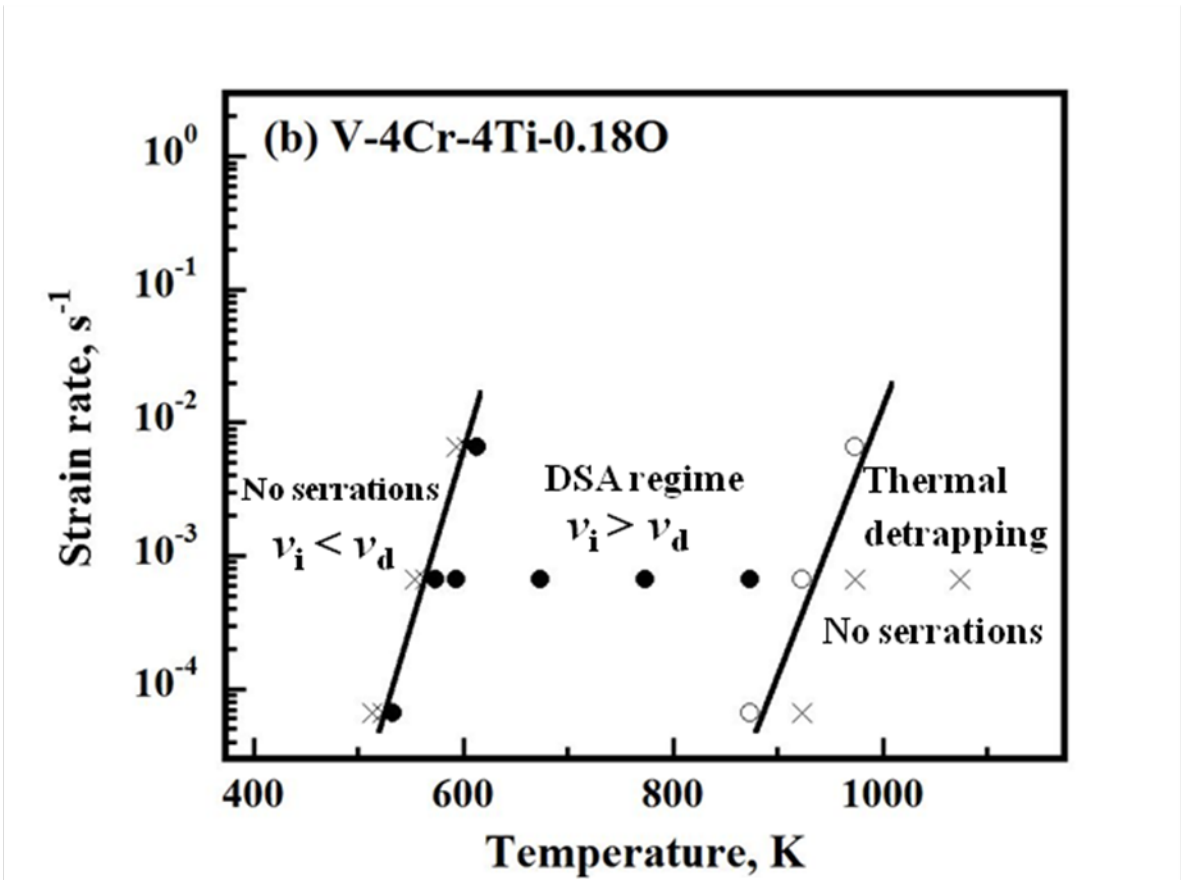
(b) V-4Cr-4Ti-0.18O
No serrations
$v_i < v_d$
DSA regime
$v_i > v_d$
Thermal detrapping
No serrations
Strain rate, s^{-1}
Temperature, K

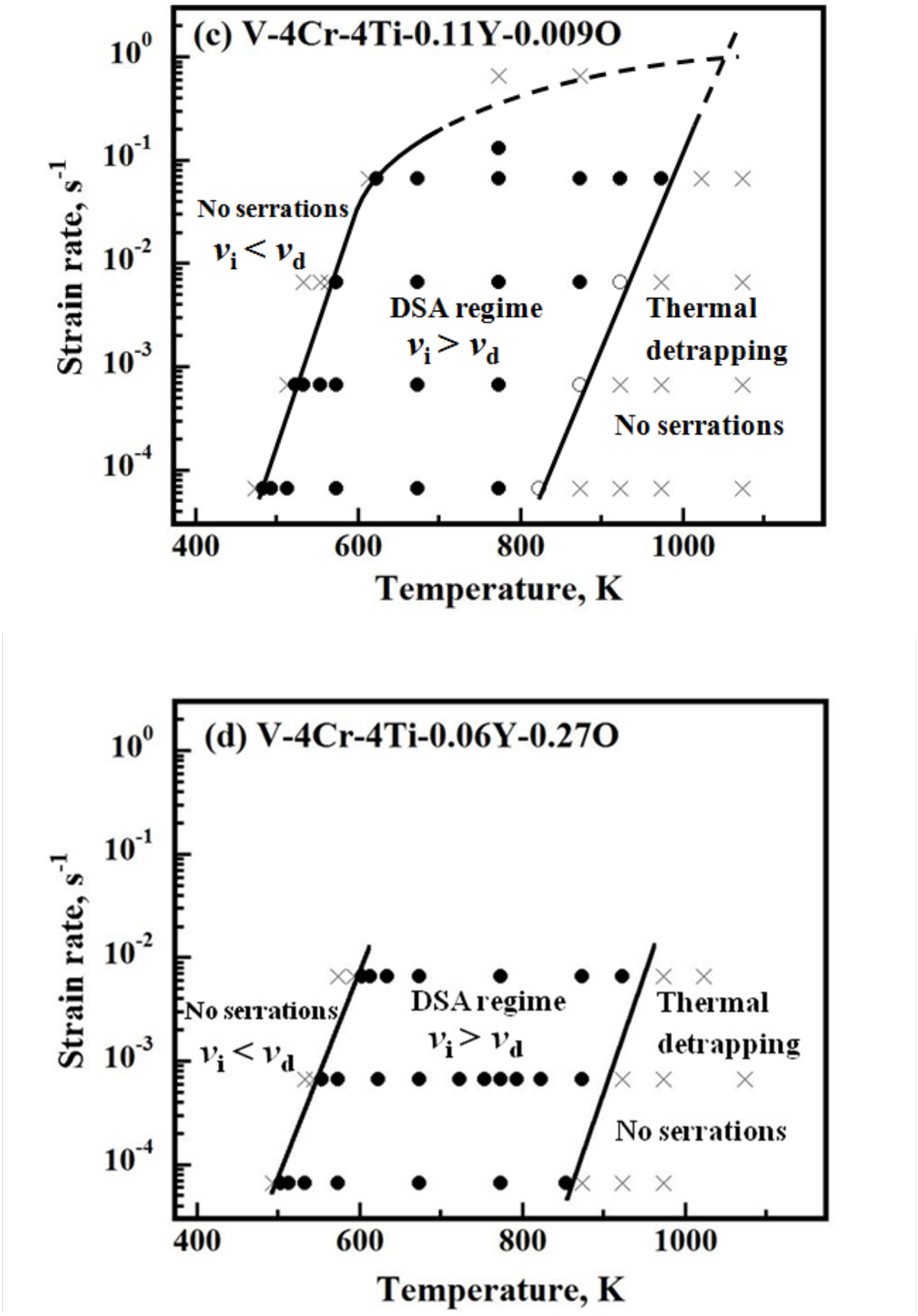

Fig. 1. DSA regimes for (a) V-4Cr-4Ti-0.019O, (b) V-4Cr-4Ti-0.18O, (c) V-4Cr-4Ti-0.11Y-0.009O

and (d) V-4Cr-4Ti-0.06Y-0.27O. Crosses show data for smooth stress-strain curves with no serrations. Closed circles show data for stress-strain curves with serrations. Open circles show data for stress-strain curves with serrations only after necking.

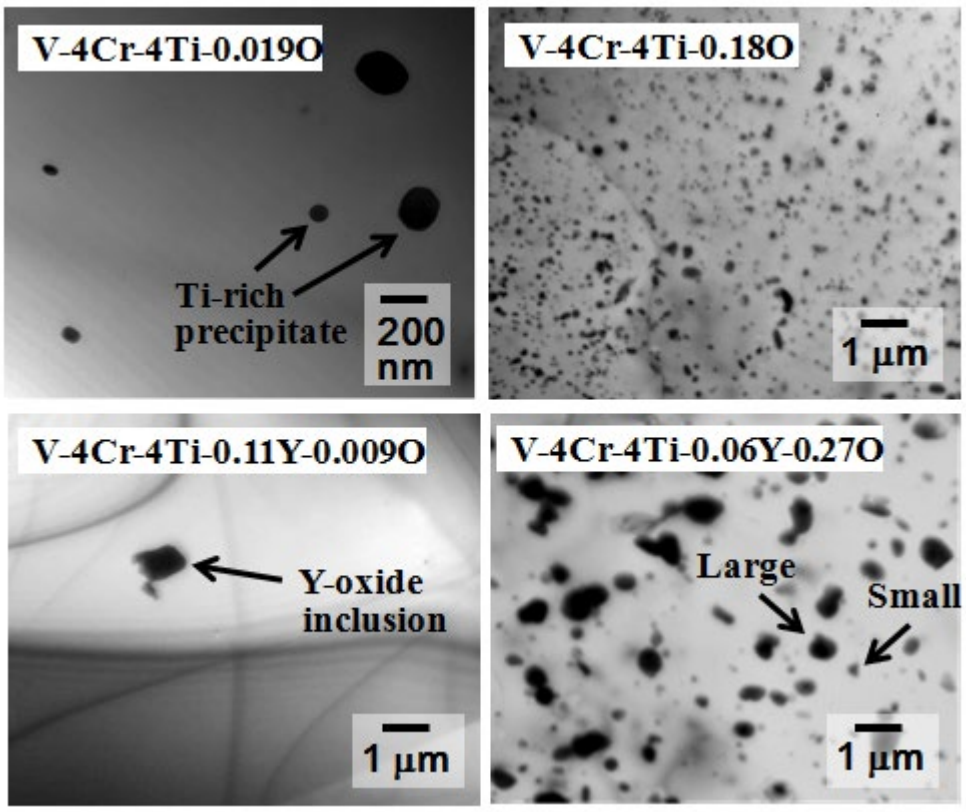

Fig. 2. TEM microstructures of the various V-4Cr-4Ti alloys examined in this study.

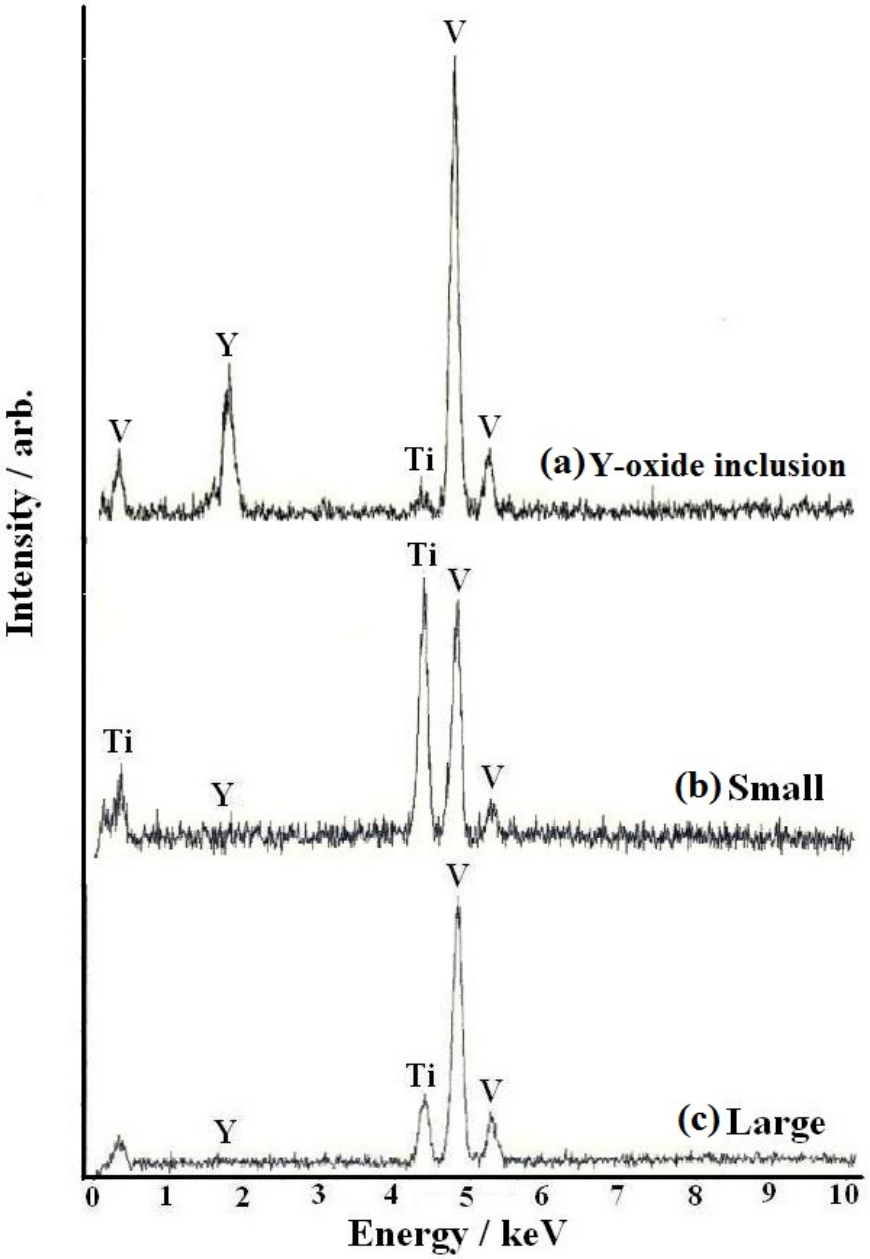

Fig. 3 TEM-EDX spectrum for (a) Y-oxide inclusion in V-4Cr-4Ti-0.11Y-0.009O, and (b) small and (c) large precipitates in V-4Cr-4Ti-0.06Y-0.27O.

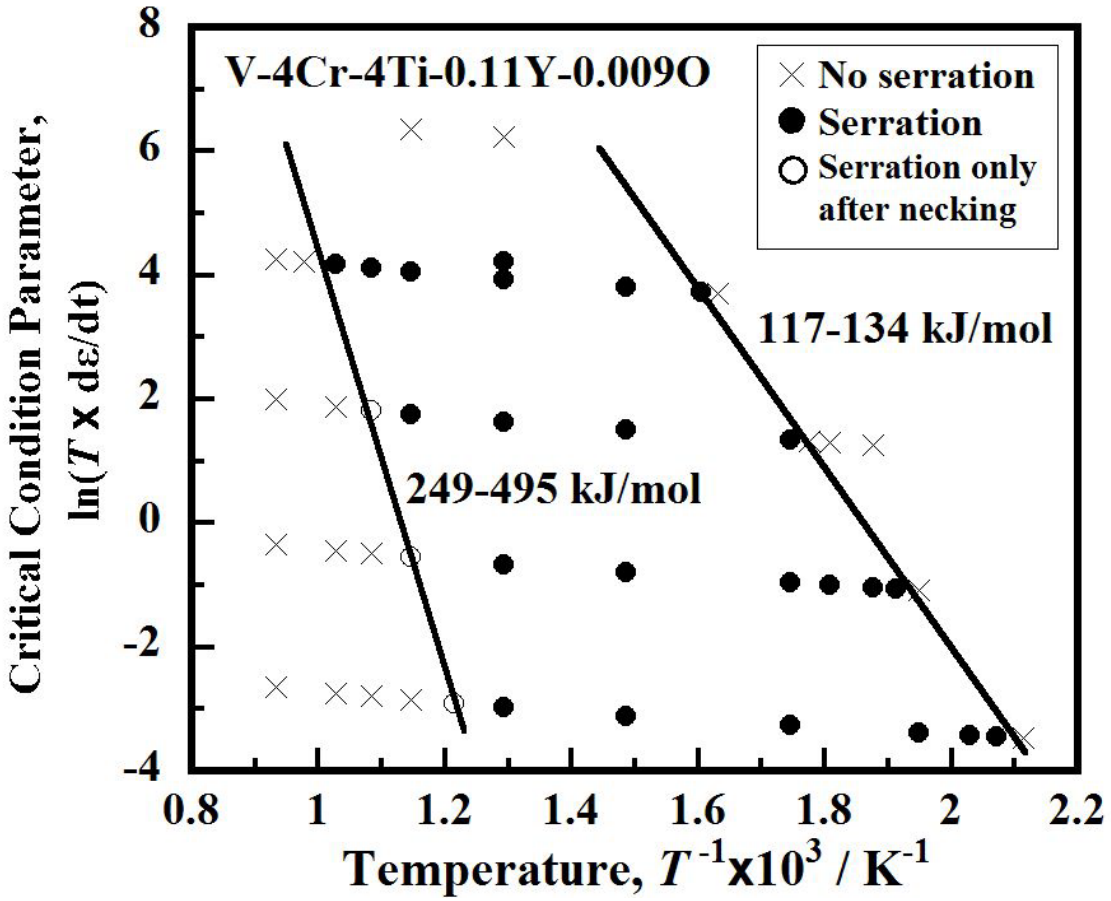

Fig. 4. Arrhenius plot of critical condition parameter ln (T x dε/dt) versus inverse absolute temperature (1000/T) for V-4Cr-4Ti-0.11Y-0.009O.